Fusion of forward-looking infrared camera and down-looking ground penetrating radar for buried target detection

Seniha Esen Yuksel[a]*, Gozde Bozdagi Akar[b], Serhat Ozturk[c]
[a]Hacettepe University, Department of Electrical and Electronics Engineering
[b]Middle East Technical University, Department of Electrical and Electronics Engineering
[c]IPA Defense Ltd., Ankara, Turkey

ABSTRACT

In this paper, we propose a system to detect buried disk-shaped landmines from ground penetrating radar (GPR) and forward-looking long wave infrared (FL-LWIR) data. The data is collected from a test area of 500m^2, which was prepared at the IPA Defence, Ankara, Turkey. This test area was divided into four lanes, each of size 25m length by 4m width and 1m depth. Each lane was first carefully cleaned of stones and clutter and then filled with different soil types, namely fine-medium sand, course sand, sandy silt loam and loam mix. In all lanes, various clutter objects and landmines were buried at different depths and at 1meter intervals. In the proposed approach, IR data is used as a pre-screener. Then possible target regions are further analyzed using the GPR data. IR data processing is done in three steps such as pre-processing, target detection, and postprocessing. In the pre-processing stage, bilateral noise reduction filtering is performed. The target detection stage finds circular targets by a radial transformation algorithm. The proposed approach is compared with the RX algorithm used widely for anomaly detection. The suspicious regions are further analyzed using Histogram of Oriented Gradient (HOG) features that are extracted from GPR images and classified by SVM. The same approach can also be applied in a parallel way where the results are combined using decision level fusion. The results of the proposed approach are given on different scenarios including different weather temperature and depth of buried targets.

Keywords: GPR, ground penetrating radar, landmine, classification, detection, thermal, long wave infrared, LWIR, FL-LWIR.

1. INTRODUCTION

Antipersonnel (AP) landmines hidden in the ground are frequently used at times of war or conflict, to restrict enemy movements. Often times, they are not removed even after the conflict is resolved. Most landmines can be functional for 50 years, and if not removed, can have a negative impact on civilian life. The clearance of a minefield is a very dangerous, costly and complex procedure and should be accomplished with very little human interaction for the sake of safety.

There are several researches reported in the literature for automated mine detection using different sensors and pattern recognition techniques [1]-[7], [23]. In these studies, considering the high sensitivity of the mine-cleaning procedures, it has become clear that one sensing technology is not enough, and several detectors' fusion is often necessary [8]- [14]. Majority of these algorithms utilize GPR data, which uses the difference in permittivity of the mine and the area surrounding it. There are also studies that use FL-LWIR data, which are based on the assumption that landmines have different thermal properties than their surrounding soil. So an indication for the presence of landmines is difference in local thermal contrast. Therefore, these two imaging modalities have complementary information, and FL-LWIR can be used in increasing the detection rates of the GPR systems.

Even though Ground Penetrating Radar (GPR) systems can give alarms for buried threats autonomously, it is ultimately the operators' responsibility to decide whether the given alarm is a mine or not. To assist the operators, in this work, a novel sensor fusion framework is proposed where a forward looking long wave infrared (FL-LWIR) camera and a down looking GPR (Niitek) mounted on the top and on the front of a robotic system, respectively, are used.

*Contact: eyuksel@ee.hacettepe.edu.tr, Phone: (+90) 312- 297 7000 / 145, Web: http://www.ee.hacettepe.edu.tr/~eyuksel/

2. LANDMINE DETECTION SYSTEM

In order to detect the landmines with a limited user assistance, a functional automated system should be used. During the experiments used in this study, an autonomous robot equipped with a forward looking long wave infrared (FL-LWIR) camera and a down looking ground penetrating radar (GPR) is used as shown in Fig. 1. The GPR is developed by Niitek (USA). It works at 0.2-7 GHZ frequency range. It records a 60cm wide area at a rate up to 20cm/sec. The panel has 12 channels and it stands 4cm above the ground. The thermal camera is a 8-14micron forward looking long wave infared (FL-LWIR) camera that records images of size 640x480. It is mounted on top of the robot at a predetermined angle looking down towards the ground. The scene of data collection as seen from the visible and thermal cameras as shown in Fig. 2. The test area is first observed by the FL-LWIR and then the GPR.

This system collected data from a test area of $500m^2$, which was prepared at the IPA Defence, Ankara, Turkey. This test area was divided into four lanes, each of size 25m length by 4m width and 1m depth. Each lane was first carefully cleaned of stones and clutter and then filled with different soil types, namely fine-medium sand, course sand, sandy silt loam (medium-course silt / medium-course sand mix) and loam mix (fine silt mixed with fine gravel). In all lanes, various clutter objects and landmines were buried at different depths and at 1meter intervals. The landmines were designed by an expert soldier; two examples are shown in Fig. 3.

Figure 1: GPR, thermal and visible cameras mounted on a robot and scanning the lanes with varying soil content.

Figure 2: The scene of data collection from the visible camera on the left, and from the thermal camera on the right. In the thermal image, disturbed earth appears to have a lighter color.

Figure 3: A close-up image of the sand and examples of AP mines.

3. FORWARD LOOKING LONG WAVE INFRARED BASED DETECTION

For forward looking infrared sensor, the goal is to locate any indicators of local thermal contrast, which may be caused by the differences in heat accumulation of the buried objects or from the presence of disturbed earth. For this purpose, two methods have been tested: (1) The global RX and the local RX algorithms that are well-known anomaly detectors, and (2) the circular shape based detection.

The baseline algorithm to detect the contrast difference in FL-LWIR images is an anomaly detector known as the Reed-Xiaoli (RX) algorithm. Global Reed-Xiaoli (RX) models the image as a Gaussian distribution with mean $\hat{\mu}$ and variance σ^2. It computes the distance between the image and a test pixel x as follows:

$$r_{GRX}(\mathbf{x}) = \frac{(\mathbf{x} - \hat{\mu})^2}{\sigma^2}$$

In essence, every pixel is tested against the global mean and variance of the image; and the test pixel is called an anomaly if this distance **r** is bigger than a threshold.

The local RX is similar to the GRX, however, instead computing the mean and the variance from the whole image, it takes a two windows and slides them over the whole image as shown in Figure 4 . The region between the inner and outer windows is considered to be the background. If the center pixel being tested is different than the background, then the distance is would be large, and the tested pixel is marked as an anomaly.

$$r_{LRX}(\mathbf{x}) = \frac{(\mathbf{x} - \hat{\mu}_{\boldsymbol{local}})^2}{\sigma^2_{local}}$$

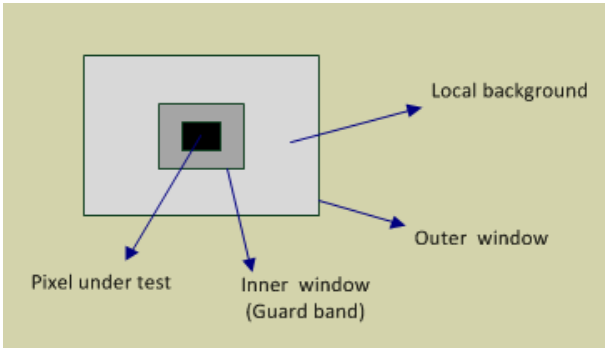

Figure 4: The local RX window showing the local background that is taken as the region between the inner and outer windows. Figure is taken from [16].

In addition to the anomaly detection approach, the shape features can also be utilized to detect landmines form FL-LWIR images [23][24]. Since we are looking for disk-shaped landmines and have a vertical imaging geometry, the images recorded should have circular shape structures. The circle detection problem has been extensively studied in the literature and many different approaches have been developed [20][21][22][23]. These approaches can be classified as accumulator based and non-accumulator based. Hough Transform (HT) is the most popular accumulator based method and it is still widely used because of its robustness against noise, clutter, object defects, shape distortions, etc.On the other hand, this method requires massive memory and excessive computation power. For efficient detection of a circle, many researches proposed modifications to the HT, [25][26]. In this work we use a noval, non accumulator based circle detection algorithm that has been previously used for circular structure detection from aerial images [27]. The main idea behind this method is reducing the search space for circle parameters in order to reduce the complexity of the algorithm by evaluating limited number of directional integrals, i.e the Radon Transform in different angles, to detect circles. Since each object is handled separately using simple transformations and the circles are detected by finding local peaks in transform domain, this new method requires much less memory and it is less computationally complex than the many of the methods found in the literature.

To test these algorithms, a target detection scenario was constructed as shown in Figure 5. Here, 9 holes were dug at 5, 10 and 15cm and landmines were placed in the first 6 holes. In the first three, landmines had been sitting outside and were cold; but the next three were recently brought in and buried after being at room temperatures. The differences are subtle yet visible to the eye. In Figure 6, Global RX results are presented after thresholding. Global RX is a fast algorithm and does not require any parameters other than the threshold at the very end. A rough threshold quickly indicates where disturbed earth is evident; however, it marks a lot of regions as anomalies.

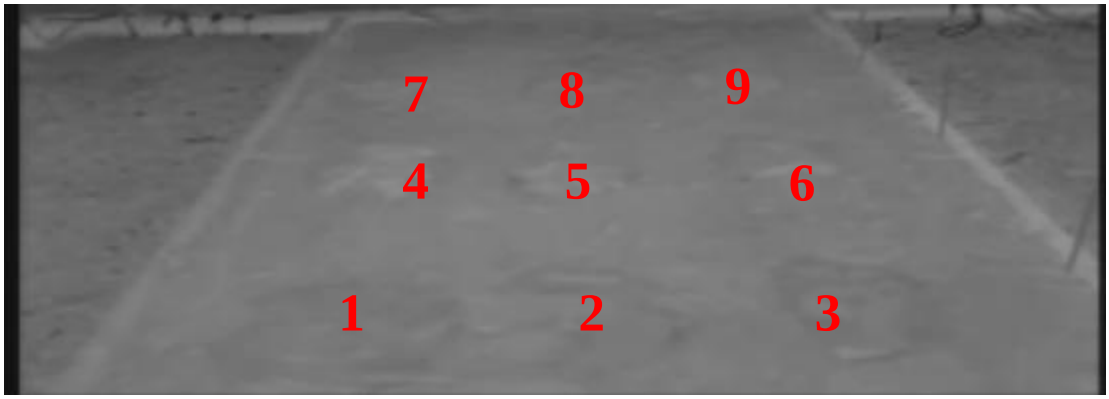

Figure 5: A scenario for target detection based on temperature and depth. Holes were digged at 5cm, 10cm and 15cm on a rather cold day (5 degrees). Then, landmines were placed on the first six holes, and the last 3 holes were covered up without placing anything in the hole. (1) Cold landmine placed at 15cm, (2) cold landmine at 10cm, (3) cold landmine at 5cm, (4) warm landmine at 15cm, (5) warm landmine at 10cm, (6) warm landmine at 5cm, (7) blank hole at 15cm (disturbed earth), (8) blank hole at 10cm and (9) blank hole at 5cm. Cold landmine is a landmine that was at the outside temperature, whereas a warm landmine has been recently buried after being at room temperature.

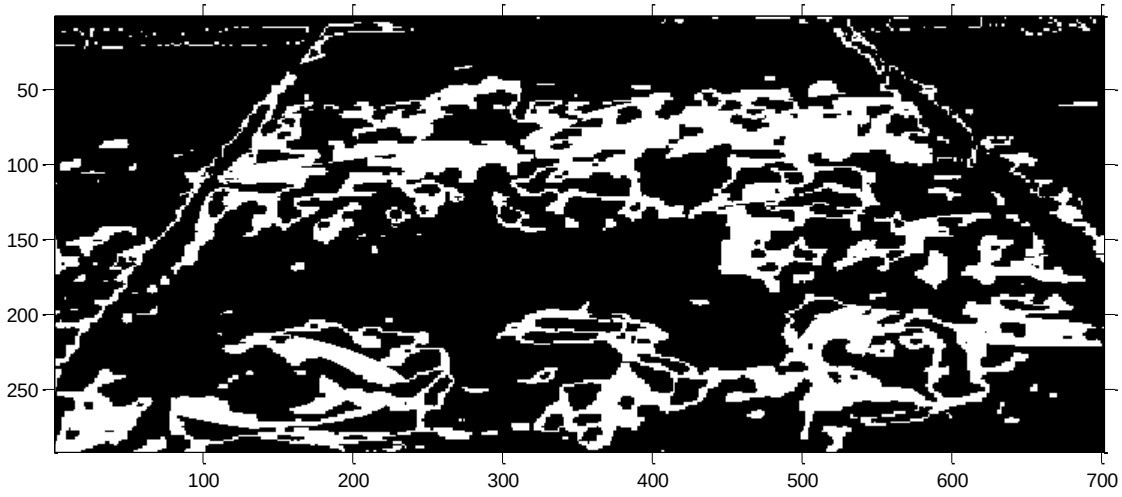

Figure 6: Global RX results after thresholding. GRX is fast and does not need any parameters; however, threshold selection may be tricky. A rough threshold quickly indicates the regions where disturbed earth is present.

As opposed to the global RX that computes the mean and variance from all of the image, local RX slides a window over the image and computes the local mean and variance values. This decreases the area of the anomaly regions as shown in **Error! Reference source not found.** and Figure 8. In the local RX, the inner window size was selected as 51 and the outer window was set to 81. Considering the oblique view of the FL-LWIR camera, window sizes were selected based on the size of the targets in the middle. In Figure 8, the local RX values from **Error! Reference source not found.** were thresholded and the threshold was selected to be the 5% of the maximum RX value. Then, in Figure 9, connected component analysis was applied and the connected components that are smaller than the outer window size were removed. The centroids of the remaining connected components are shown in Figure 10 as red dots overlayed on the landmines shown with the ellipses. Red dots falling outside the ellipses are false alarms.

The same scene is also analyzed by the utilized circle detection algorithm. The edges on the binarized image is detected and for a the projections of each connected component is analyzed to be a circle or not. The results of the algorithm is shown in Figure 11 where the centroids of the circles are shown.

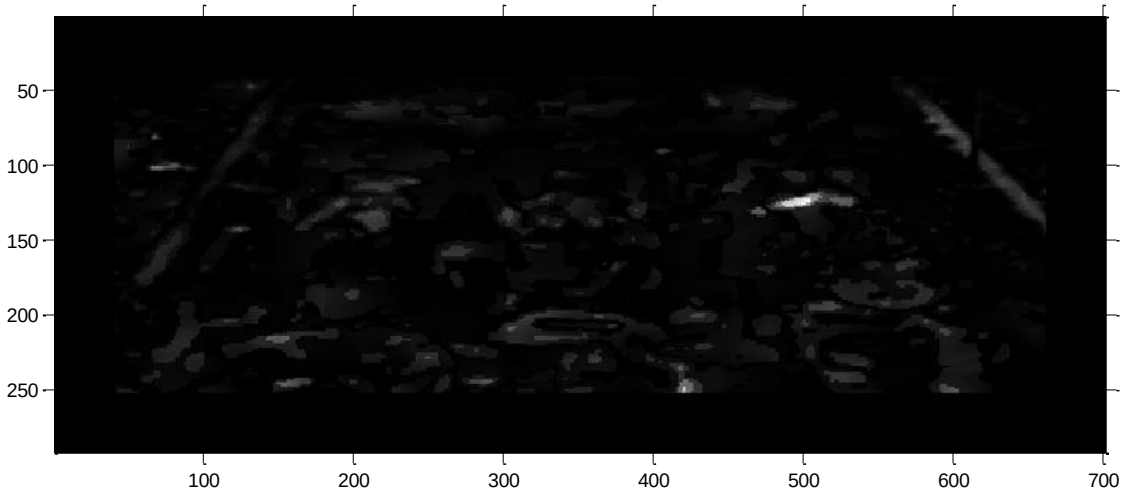

Figure 7: Local RX results. The inner window was set to 51 and the outer window was set to 81. Due to the oblique view, window sizes were selected considering the size of the targets in the middle.

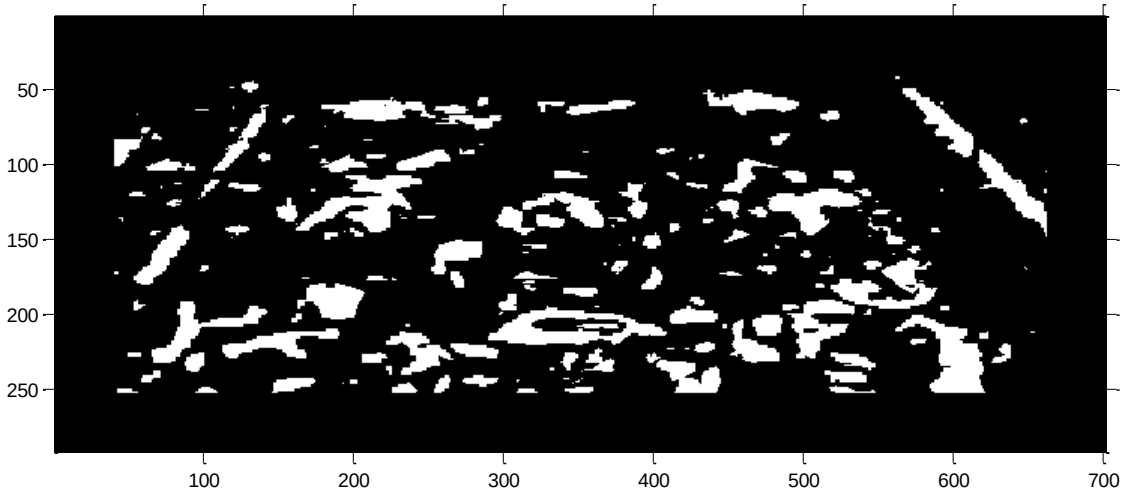

Figure 8: Thresholding the local RX values. Threshold was set to be the 5% of the maximum RX value.

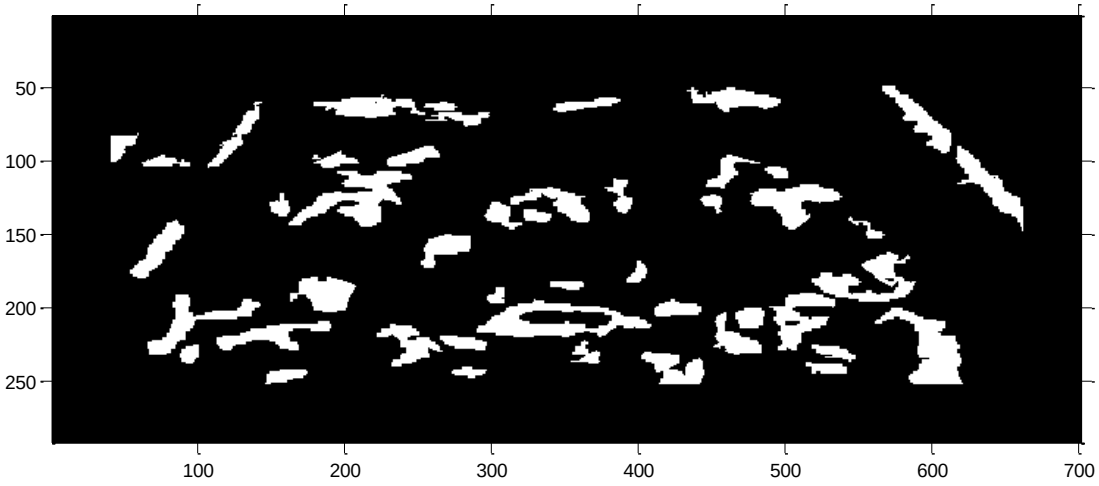

Figure 9: Connected component analysis and removal of the small components. The connected components that are smaller than the outer window size of the RX algoritm were removed.

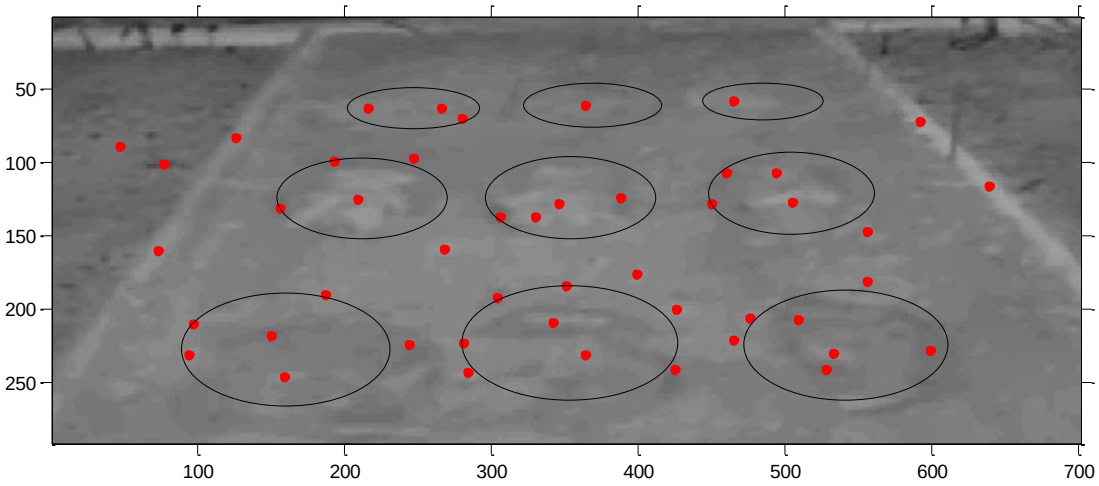

Figure 10: Centroids of the connected components are shown in red dots, whereas the locations of the landmines are shown with the ellipses. Red dots falling outside the ellipses are false alarms.

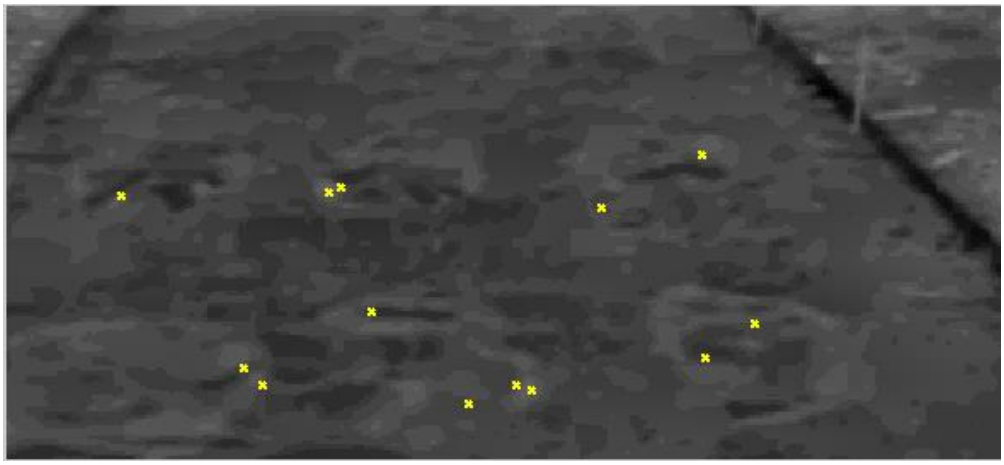

Figure 11: Centroids of the detected circles.

During this data acquisition, the weather was around 5^0 Celcius, it had recently snowed and the soil was still wet. With such weather, we did not see any indication of detecting the actual buried objects or major thermal contrast resulting from the material properties. The soil was mostly frozen and very hard to even dig. However, any small disturbance on the surface did bring the wet soil to the surface and showed a clear disturbed earth signature. Considering that detection by GPR is also not so easy under such frozen soil, these results indicate that disturbed earth might be a good indicator for landmine detection and LWIR camera can be of help as a preprocessor for GPR.

4. GROUND PENETRATING RADAR BASED DETECTION

The robotic system collected data on this lane using the GPR panel. As a complementary information to the disturbed earth characteristics of the FL-LWIR detection, the downward looking GPR provided signals from the buried objects. This GPR data was first processed using the common techniques as described and used in [1]-[6]. It was first filtered with a median filter to get rid of the GPS interference, and then ground-bounce alignment was applied followed by ground-bounce removal. Finally, whitening was applied to each time sample to make the deep and shallow time samples comparable. Each of these steps is illustrated in Figure .

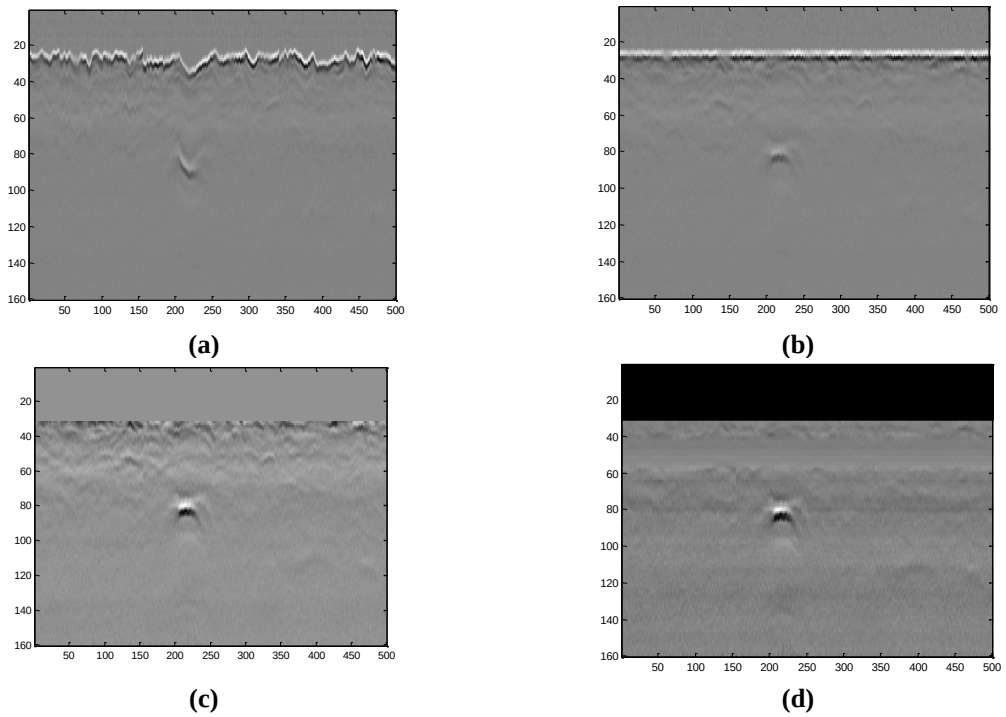

Figure 12: GPR preprocessing stages. (a) Original GPR data, (b) Ground alignment, (c) Ground bounce removal, (d) Whitening. The landmine becomes progressively apparent with each preprocessing stage. In the last stage, it has a hyperbolic signature.

Following the preprocessing, Histogram of Oriented Gradients (HOG) features were extracted from GPR data [7]. HOG descriptors explain an image using the histogram of intensity gradients and edge directions. The image is divided into small overlapping regions, called cells, and the histograms are computed for these regions. The combination of these histograms represents the descriptor. Further, to improve the accuracy, these locally computed histograms are contrast-normalized using larger regions of the image, called blocks. In doing so, the descriptors have better invariance to changes in illumination.

A typical HOG computation is based on 4 steps:

1- Gaussian smoothing is applied if the image is noisy.
2- Gradient values are computed using the two filters [-1, 0, 1] and $[-1, 0, 1]^T$.
3- Orientation binning: Orientations are found from the gradient values, and are used to form orientation histograms.
4- Block normalization: Larger regions, called blocks, are used to contrast-normalize the histograms. The histograms when concatenated together form the HOG descriptors.

In this work, VLFeat [17] libraries were used to implement the HOG descriptors. Nine histogram bins were computed per cell, with angles in the range [-pi,pi]. The HOG features for landmine and background structures are shown in Fig. 13.

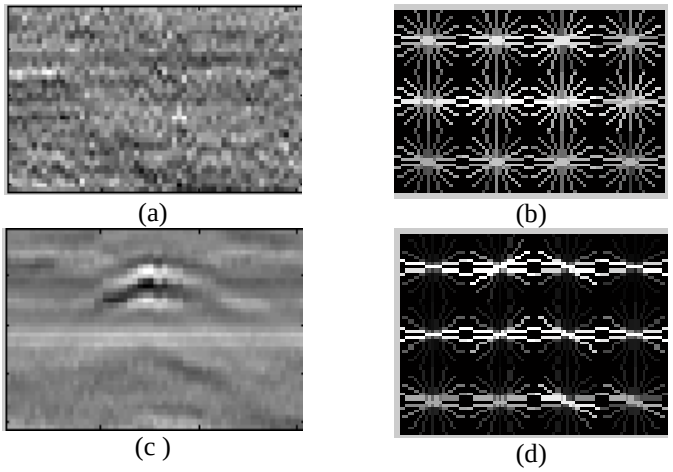

Fig 13: (a) Background data, (b) The HOG features for (a), (c) Landmine data, (d) The HOG features for (c).

GPR data was collected continuously from a lane. Each downtrack run on a line is about 20meters. On several lane data obtained on various day, certain windows were labelled as mine, background and mine-like-background. For each label group, 20 windows were selected as training data. HOG features were extracted from these windows and were used in training an SVM classifier[19]. SVM is a binary classifier which looks for an optimal hyperplane as a decision function. Therefore, to train a 3-class SVM, one-versus-all strategy was used. Examples of the training data are shown in Fig. 14 and Fig. 15 for all 3 classes.

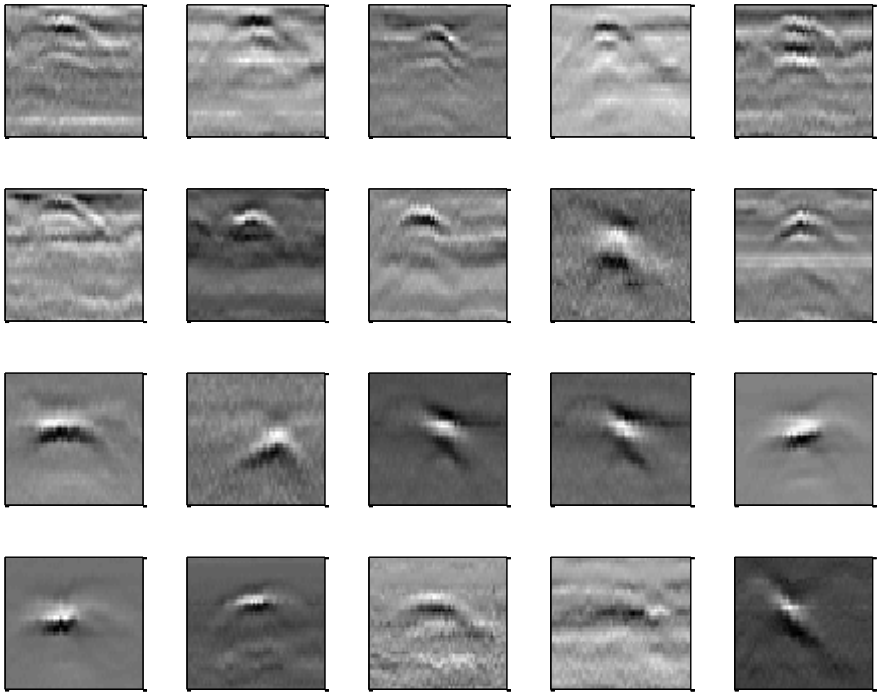

Figure 14: Examples from the training set for the mine class

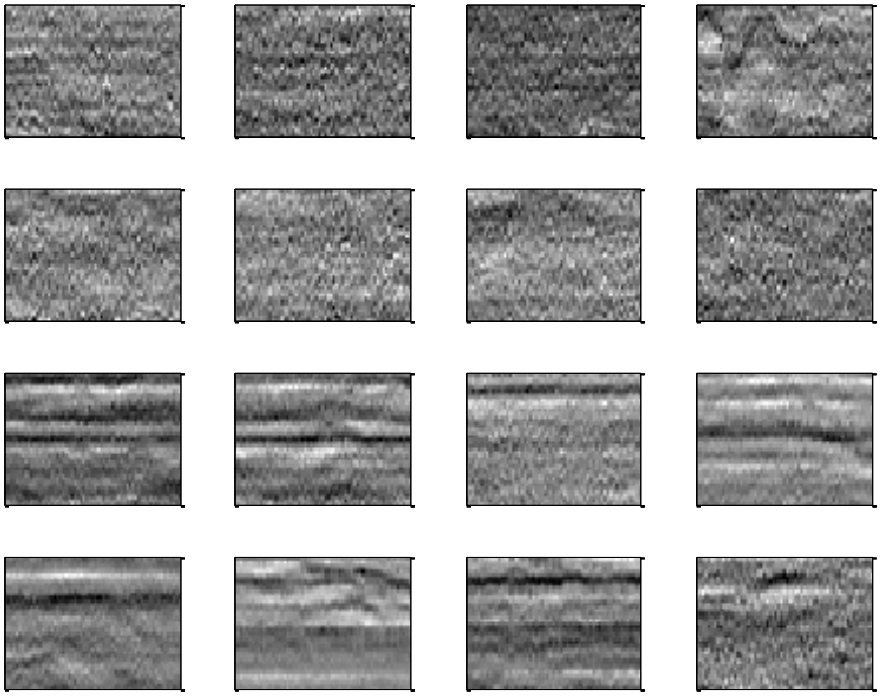

Figure 15: Examples from the training set for the background and mine-like-background classes.

For testing the classifier, 5 downtrack lane images, previously unseen, which correspond to about 120m of data were used. In the test scenario, starting from the top-left part of the GPR image, overlapping windows were slided over the entire image and for each window; firstly, HOG features were extracted and after that these features were classified by the multi-SVM. The actual landmine positions and the regions marked by the SVM as landmines are shown in Fig. 16.

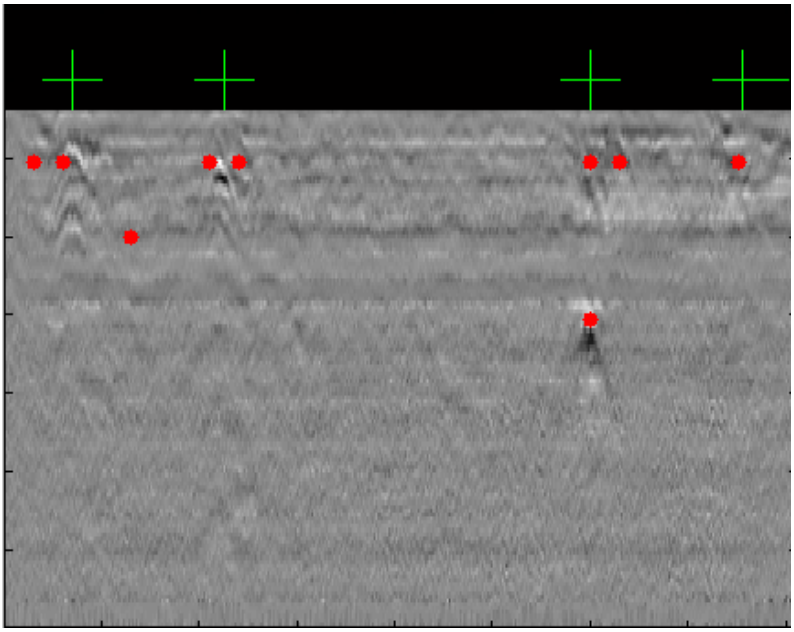

Fig 16. Detected landmines, green showing the groundtruth data, red showing the results of the detection.

5. EXPERIMENTAL RESULTS

As a last step of the proposed work, the results are obtained by cascaded FL-LWIR and GPR analysis. As stated before, the suspicious regions detected by FL-LWIR are further analyzed using the GPR data. The GPR and FL-LWIR data are initially registered. Fig 17(a) show the results of the FL-LWIR detection which is used as a prescreener. Within this detected region, the results of the GPR data analysis is shown in Fig.17.

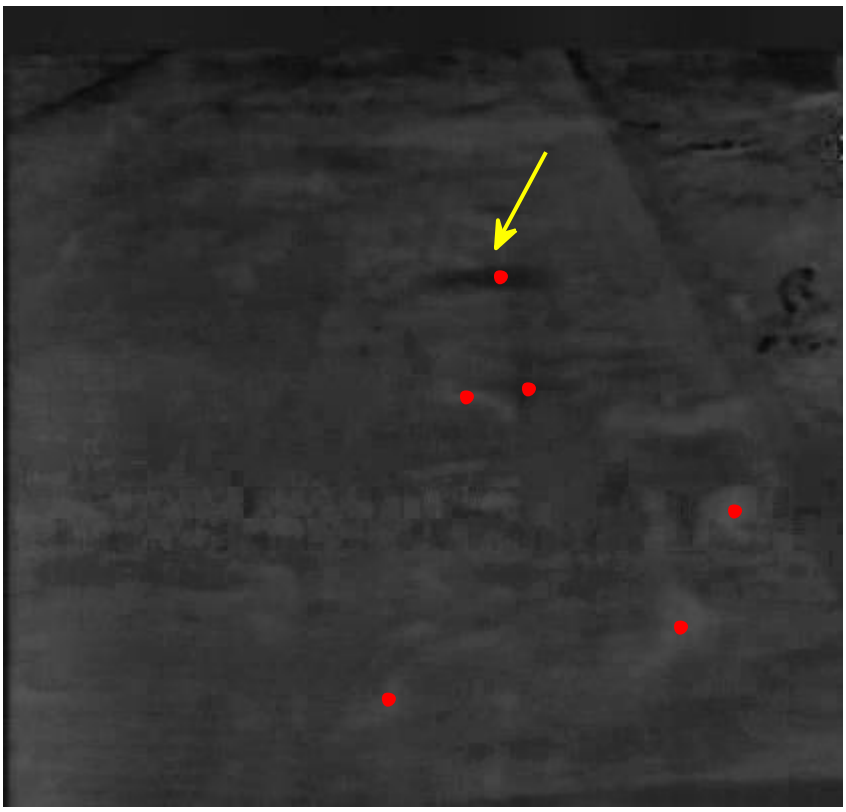

(a) FL-LWIR results: the dark region indicated with the yellow arrow is the location of the landmine. Red points are the alarms found by local RX.

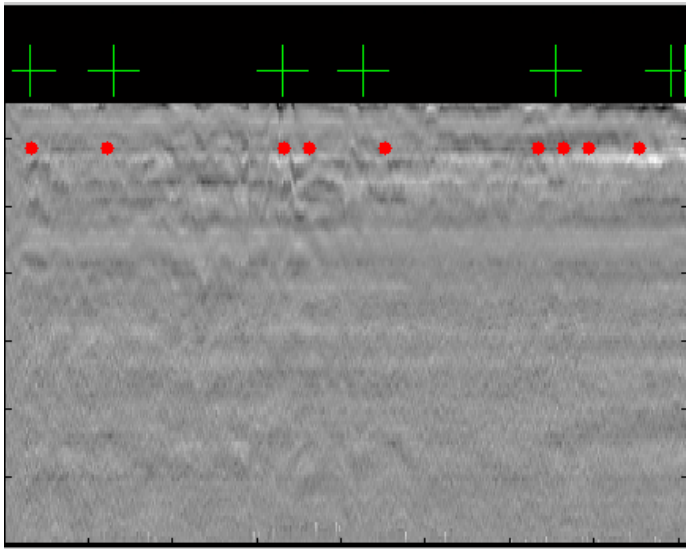

(b) Green + symbols indicate the location of landmines as a strip. Red points indicate the alarms found by GPR detection algorithm.

Fig. 17. The FL-LWIR and GPR detection results.

6. CONCLUSION

In this paper, we propose a system to detect buried disk-shaped landmines from the collected GPR and IR data. The data is collected from a test area of 500m^2, which was prepared at the IPA Defence, Ankara, Turkey. The proposed approach is two-step. First FL-LWIR data is analyzed by two different algorithms to detect disturbances. The detected regions are further analyzed using Histogram of Oriented Gradient (HOG) features that are extracted from GPR images and classified by SVM. As a future study, we plan to apply these algorithms in a parallel way where the results are combined using decision level fusion.

7. ACKNOWLEDGEMENT

We would like to thank Fırat Gürbüz for his help in the data acquisition and early data processing.

REFERENCES

[1] P. Gader, M. Mystkowski, and Y. Zhao, "Landmine detection with ground penetrating radar using hidden markov models," Geoscience and Remote Sensing, IEEE Transactions on, vol. 39, pp. 1231-1244,June 2001.

[2] Gader, P., Lee, W.H., Wilson, J.N.: ‘Detecting Landmines With Ground-Penetrating Radar Using Feature-Based Rules, Order Statistics, and Adaptive Whitening’, 2004

[3] Torrione, P., Collins, L., Clodfelter, F., Frasier, S., Starnes, I.: ‘Application of the LMS Algorithm to Anomaly Detection Using the Wichmann/Niitek Ground Penetrating Radar’,SPIE Proceedings Vol. 5089, 2003

[4] P. Torrione, C. Throckmorton, and L. Collins, "Performance of an adaptive feature-based processor for a wideband ground penetrating radar system," Aerospace and Electronic Systems, IEEE Transactions on, vol. 42, pp. 644-658, April 2006.

[5] S.E. Yuksel, J. Bolton, P. Gader, "Landmine Detection With Multiple Instance Hidden Markov Models ", IEEE International Workshop on Machine Learning For Signal Processing (MLSP) , pp. 1-6, September 2012.

[6] S.E. Yuksel, P. Gader, "Mixture of HMM Experts with Applications to Landmine Detection", IEEE International Geoscience and Remote Sensing Symposium (IGARSS) , pp. 6852 – 6855, July 2012.

[7] Torrione, P.A.; Morton, K.D.; Sakaguchi, R.; Collins, L.M., "Histograms of Oriented Gradients for Landmine Detection in Ground-Penetrating Radar Data," Geoscience and Remote Sensing, IEEE Transactions on , vol.52, no.3, pp.1539,1550, March 2014

[8] S.E. Yuksel , G. Ramachandran, P. Gader, J. Wilson, D. Ho, G. Heo, "Hierarchical methods for landmine detection with wideband electro-magnetic induction and ground penetrating radar multi-sensor systems," IEEE International Geoscience and Remote Sensing Symposium (IGARSS) , vol.2, pp. 177-180, 7-11 July 2008.

[9] S.E. Yuksel , P. Gader, "Variational Mixture of Experts for Classification with applications to landmine detection ", International Conference on Pattern Recognition (ICPR) , pp. 2981- 2984, 2010.

[10] K. Stone ; J. Keller ; K. C. Ho ; M. Busch ; P. D. Gader; On the registration of FLGPR and IR data for a forward-looking landmine detection system and its use in eliminating FLGPR false alarms. Proc. SPIE 6953, Detection and Sensing of Mines, Explosive Objects, and Obscured Targets XIII, 695314 (April 14, 2008).

[11] K. Stone ; J. M. Keller ; D. T. Anderson ; D. B. Barclay; An automatic detection system for buried explosive hazards in FL-LWIR and FL-GPR data. Proc. SPIE 8357, Detection and Sensing of Mines, Explosive Objects, and Obscured Targets XVII, 83571E (May 1, 2012)

[12] Martin Fritzsche ; Otto Loehlein; Sensor fusion for the detection of land mines. Proc. SPIE 3752, Subsurface Sensors and Applications, 414 (October 15, 1999)

[13] K. Stone ; J. M. Keller ; M. Popescu ; C. J. Spain; Buried explosive hazard detection using forward-looking long-wave infrared imagery. Proc. SPIE 8017, Detection and Sensing of Mines, Explosive Objects, and Obscured Targets XVI, 801725 (May 23, 2011).

[14] Brian Tuomanen ; Kevin Stone ; Timothy Madison ; Mihail Popescu ; James Keller; Buried target detection in FLIR images using Shearlet features. Proc. SPIE 8709, Detection and Sensing of Mines, Explosive Objects, and Obscured Targets XVIII, 870919 (June 7, 2013).

[15] Michael Theodore Eismann, “Hyperspectral remote sensing,” SPIE, 2012.

[16] Irving S Reed and Xiaoli Yu, “Adaptive multiple-band cfar detection of an optical pattern with unknown spectral distribution,” Acoustics, Speech and Signal Processing, IEEE Trans. on, vol. 38, no. 10, pp. 1760–1770,1990.
[17] Sefa Kucuk, S. E. Yuksel, Comparison of RX-Based Anomaly Detectors On Synthetic And Real Hyperspectral Data, IEEE Workshop on Hyperspectral Image and Signal Processing: Evolution in Remote Sensing (Whispers), June 2015.
[18] A. Vedaldi and B. Fulkerson, VLFeat: An Open and Portable Library of Computer Vision Algorithms, 2008. Online: http://www.vlfeat.org/
[19] Cortes, C.; Vapnik, V. (1995). "Support-vector networks". Machine Learning 20 (3): 273.
[20] S. H. Chiu and H. H. Liaw, "An effective voting method for circle detection," *Pattern Recognition Letters*, vol. 26, pp. 121-133, JAN 15 2005.
[21] [6] D. Ioannou, *et al.*, "Circle recognition through a 2D Hough Transform and radius histogramming," *Image and Vision Computing*, vol. 17, pp. 15-26, JAN 1999.
[22] D. Walsh and A. E. Raftery, "Accurate and efficient curve detection in images: the importance sampling Hough transform," *Pattern Recognition*, vol. 35, pp. 1421-1431, Jul 2002.
[23] W. A. C. M. Messelink, K. Schutte, A. M. Vossepoel, F. Cremer, J. G. M. Schavemaker, and E. D. Breejen, "Feature-based detection of landmines in infrared images," In the Proceedings of the SPIE- detection and remediation technology for mine and minelike targets VII, Vol. 4742, 2002, pp 1-12
[24] Bai Kunth Nath and A.Bhuiyan, "A geometrical feature based sensor fusion model of GPR and IR for the detection and classification of anti-personnel mines,"IEEE Computer Society, pp.849-856,2007.
[25] K. L. Chung and Y. H. Huang, "Speed up the computation of randomized algorithms for detecting lines, circles, and ellipses using novel tuning- and LUT-based voting platform," Applied Mathematics and Computation, vol. 190, pp. 132-149, Jul 1 2007.
[26] J. Wu, K. Chen, and X. Gao, “Fast and accurate circle detection using gradient-direction-based segmentation,” J. Opt. Soc. Am. A 30, 1184–1192 (2013).
[27] O. E. Okman, G. B. Akar, “A circle detection approach based on Radon Transform”, Proc. ICASSP, 2013.